Publication Year	2022
Acceptance in OA	2022-03-22T14:19:25Z
Title	The Evolution of AGN Activity in Brightest Cluster Galaxies
Authors	Somboonpanyakul, T., McDonald, M., Noble, A., Aguena, M., Allam, S., Amon, A., Andrade-Oliveira, F., Bacon, D., Bayliss, M. B., Bertin, E., Bhargava, S., Brooks, D., Buckley-Geer, E., Burke, D. L., Calzadilla, M., Canning, R., Carnero Rosell, A., Carrasco Kind, M., Carretero, J., Costanzi, M., da Costa, L. N., Pereira, M. E. S., De Vicente, J., Doel, P., Eisenhardt, P., Everett, S., Evrard, A. E., Ferrero, I., Flaugher, B., Floyd, B., García-Bellido, J., Gaztanaga, E., Gerdes, D. W., Gonzalez, A., Gruen, D., Gruendl, R. A., Gschwend, J., Gupta, N., Gutierrez, G., Hinton, S. R., Hollowood, D. L., Honscheid, K., Hoyle, B., James, D. J., Jeltema, T., Khullar, G., Kim, K. J., Klein, M., Kuehn, K., Lima, M., Maia, M. A. G., Marshall, J. L., Martini, P., Melchior, P., Menanteau, F., Miquel, R., Mohr, J. J., Morgan, R., Ogando, R. L. C., Palmese, A., Paz-Chinchón, F., Pieres, A., Plazas Malagón, A. A., Reil, K., Romer, A. K., Ruppin, F., Sanchez, E., SARO, ALEXANDRO, Scarpine, V., Schubnell, M., Serrano, S., Sevilla-Noarbe, I., SINGH, PRIYANKA, Smith, M., Soares-Santos, M., STRAZZULLO, VERONICA, Suchyta, E., Swanson, M. E. C., Tarle, G., To, C., Tucker, D. L., Wilkinson, R. D.
Publisher's version (DOI)	10.3847/1538-3881/ac5030
Handle	http://hdl.handle.net/20.500.12386/31787
Journal	THE ASTRONOMICAL JOURNAL
Volume	163

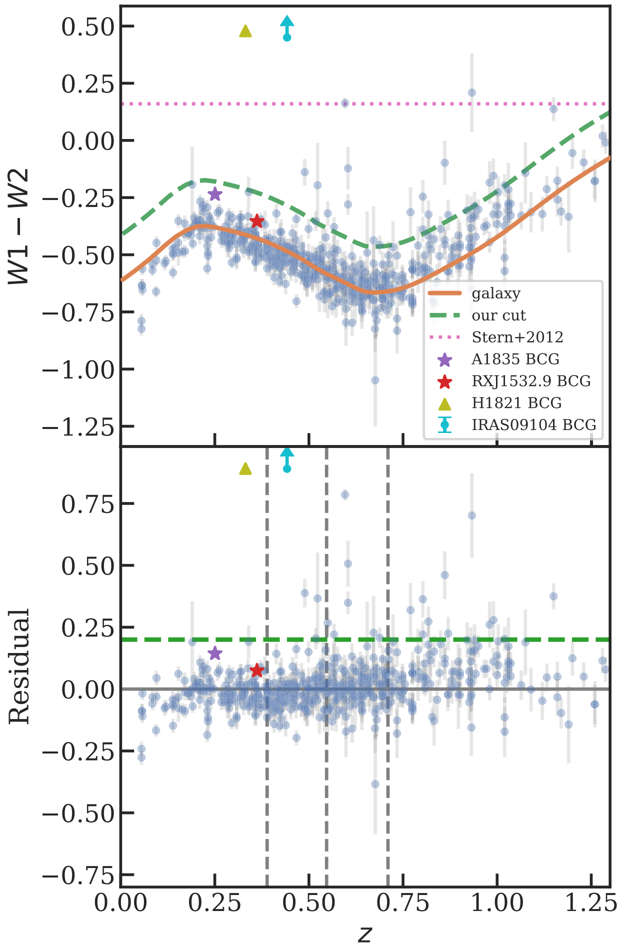

Figure 3. Top: $W1$–$W2$ color for each BCG candidate as a function of cluster redshift. The solid orange line shows the expected color as a function of redshift for our elliptical galaxy model using EzGal, as described in Section 3.1.1. The dashed green line shows our criterion for selecting AGNs, which is derived from the orange line, and the dotted pink line shows the cut from the previous work by Stern et al. (2012). Bottom: the $W1$–$W2$ color difference between each BCG candidate and the expected color. The dashed green line shows our selection with the residual >0.2. Every object with a residual greater than 0.2 is likely to be an AGN. The vertical dashed gray lines show the binning for the results in Figure 6. The redshift bins are defined such that each bin contains roughly the same number of systems, making for uniform counting statistics across all redshifts. The two colored stars are known BCGs in galaxy clusters with a high SFR, showing that our selection criterion does not select these starburst BCGs, while the two clusters with luminous AGNs (H 1821+643 and IRAS 09104+4109) are clearly above our criterion.

and projecting them through filters (Mancone & Gonzalez 2012). This calculation takes into account both the stellar evolution of a galaxy as young stars evolve and the wavelength shift due to the distance of a galaxy. To find the model that best describes our overall sample, we perform a grid search between three stellar population model sets (i.e., Bruzual & Charlot 2003; Maraston 2005; Conroy et al. 2009), various formation redshifts, two different initial mass functions (IMF) (i.e., Salpeter 1955; Chabrier 2003), star formation history as a single exponential decaying burst of star formation with an e-folding time parameter (τ) between 0.1 and 10 Gyr, and the representative metallicity (Z) for our galaxy sample from 0.001 to 0.03. Ultimately, the best-fit model (based on the chi-square test) is a Bruzual & Charlot (2003) stellar model with a formation redshift of (z_f) 3.5, a Salpeter (1955) IMF, $\tau = 0.1$ Gyr for the star formation history, and a metallicity of 0.016. The solid orange line in the top panel of Figure 3 shows the expected $W1$–$W2$ color evolution, generated from the EzGal model with this particular set of parameters. The bottom panel shows the residual from the expected value of $W1$-$W2$ for each BCG. It demonstrates that the scatter is distributed around zero with a relatively weak redshift dependence, implying that we have successfully removed the continuum contribution. In this work, galaxies that are redder (a residual greater than 0.2) than typical elliptical galaxies based on the EzGal model are considered AGN candidates. For a range of threshold values from 0.2 to 0.4, the highest redshift bin has more AGN-hosting BCG sthan the lowest redshift bin, implying that an increase in the fraction of AGN-hosting BCGs is independent of this choice. To further test this notion, we perform a heteroscedasticity test, specifically, the Breusch-Pagan test, in the bottom panel of Figure 3, which shows whether the scatter of the IR residual depends on redshift, regardless of the choice of a threshold value. The test results in a P-value = 0.0047, meaning that the heteroscedasticity is present and the scatter of $W1$–$W2$ residuals depends on the redshift, implying that an increase in the fraction is feasible regardless of the threshold choice.

One assumption that we apply in this section is that we only consider a single-burst stellar population model with a single formation redshift, star formation history, and metallicity. In Figure 4 we consider both a single-burst stellar population model and a more complicated two-age stellar population (old and young) model with a wide range of parameters for both models. The model with two stellar populations keeps the same parameter sets from a single-burst model for the "old" population, while a "young" population is represented by a 50 Myr old stellar population at all redshifts. Even though these two models are likely not sufficient to describe our data, more sophisticated models would be unconstrained by the data that we have available. Based on these single-age and two-age models, we find no combination of formation time, metallicity, and IMF that can fully account for the observed evolution in the mid-IR excess, as shown in the right panel of Figure 4. We propose that this mid-IR excess comes from a dusty torus, which is a signature of an actively accreting SMBH. It is difficult to imagine other astronomical sources for this emission because star formation typically yields significantly cooler dust temperatures with a peak brightness of $\sim$100 μm instead of $\sim$1–10 μm. On the other hand, it could also be that our current population models are not adequate to describe the data. We should keep this caveat in mind when we discuss the implication of our results.

As a test to see how a starburst can affect the mid-IR color, we consider Abell 1835 (Ehlert et al. 2011) and RX J1532.9+3021 (Hlavacek-Larrondo et al. 2013), which are the most star-forming BCGs known (SFR $\sim 100\, M_\odot\, \mathrm{yr}^{-1}$; McDonald et al. 2018) that also lack evidence of a strong AGN. The two colored stars in Figure 3 demonstrate that even though a star-forming BCG would have boosted mid-IR emission due to dust, polycyclic aromatic hydrocarbon molecules (PAH), and molecular gas, the emission is not as strong as the power-law spectra of AGNs, and our selection does not include these two BCGs. On the other hand, the two clusters with the most luminous AGNs (H 1821+643; Russell et al. 2010, and IRAS 09104+4109; O'Sullivan et al. 2012) are easily detected with our criterion.